

NJC

Accepted Manuscript



This is an *Accepted Manuscript*, which has been through the Royal Society of Chemistry peer review process and has been accepted for publication.

Accepted Manuscripts are published online shortly after acceptance, before technical editing, formatting and proof reading. Using this free service, authors can make their results available to the community, in citable form, before we publish the edited article. We will replace this *Accepted Manuscript* with the edited and formatted *Advance Article* as soon as it is available.

You can find more information about *Accepted Manuscripts* in the [Information for Authors](#).

Please note that technical editing may introduce minor changes to the text and/or graphics, which may alter content. The journal's standard [Terms & Conditions](#) and the [Ethical guidelines](#) still apply. In no event shall the Royal Society of Chemistry be held responsible for any errors or omissions in this *Accepted Manuscript* or any consequences arising from the use of any information it contains.

LETTER

Metal-metal bond passing through the arene ligand: Theoretical study on inverse sandwiches $X[\text{Sc-C}_8\text{H}_8\text{-Sc}]_nX$ ($X = \text{F, Cl, Br}$; $n = 1, 2$)

Cite this: DOI: 10.1039/c3nj00000x

Nan N. Liu,^{a,*} and Yi H. Ding^{b,*}Received 00th XXXXX 2013,
Accepted 00th XXXXX 2013

DOI: 10.1039/c3nj00000x

www.rsc.org/njc

The Sc-Sc bond through the hole of C_8H_8 in $X[\text{Sc-C}_8\text{H}_8\text{-Sc}]X$ ($X = \text{F-Br}$), and the uninterrupted Sc-Sc bond-chain with both the Sc-Sc bond through C_8H_8 and the Sc-Sc bond between two $[\text{Sc-C}_8\text{H}_8\text{-Sc}]$ units in $X[\text{Sc-C}_8\text{H}_8\text{-Sc}]_2X$ are predicted. The molecules are roughly estimated as potential electro-conductive by the low HOMO-LUMO gaps.

Inverse sandwiches refer to complexes with the bipyramidal structure of two metal atoms on opposite sides of an arene ligand. Since the $[\text{Ga-Cp}^+\text{-Ga}]^+$ cation with Ga(I) was successfully synthesized as the fully ionized $[\text{B}(\text{C}_6\text{H}_3(\text{CF}_3)_2)_4]^-$ salt,¹ more attention was focused on the particular properties of inverse sandwiches to stabilize the metals with unusual valences, e.g. Ca(I), U(V), Cr(I) and mixed-valent Ti(I)/Ti(II) in their triphenylbenzene, toluene, benzene and toluene complexes,²⁻⁵ respectively. More chemical properties of inverse sandwiches were predicted by theoretical investigations, such as $[\text{Mg-Si}_5\text{H}_5\text{-Mg}]^{3+}$ with flattened Si_5 ring, $\text{Ca-C}_4\text{H}_4\text{-Ca}$ with NLO properties, $\text{Ca-C}_8\text{H}_8\text{-Ca}$ with singlet diradical character, and etc..⁶⁻¹⁰ Noted that although $\text{Ca-C}_8\text{H}_8\text{-Ca}$ is a singlet diradical, the complex $(\text{DME})_3\text{Ca-C}_8\text{H}_8\text{-Ca}(\text{DME})_3$ (DME = dimethyl ether) contains a direct Ca-Ca interaction through the C_8H_8 ligand.¹⁰ The bond through the arene ligand might be an important property for inverse sandwiches. Assuming a molecular wire consisting of inverse sandwich unites with metal-metal bond through the ligand or even with the metallic bond-chain, it would be a potential conductive material. Then, it is of interest to develop this type of inverse sandwiches.

Herein, we performed a theoretical study on inverse sandwiches $X[\text{Sc-C}_8\text{H}_8\text{-Sc}]_nX$ ($X = \text{F, Cl, Br}$; $n = 1, 2$) with potential Sc-Sc interaction. Different from the $4s^2$ electron configuration of calcium, the $4s^23d^1$ configuration gives scandium atoms have sufficient valence to form not only the Sc-Sc bond through the ligand, but also the Sc-Sc bond between two $[\text{Sc-C}_8\text{H}_8\text{-Sc}]$ units in $X[\text{Sc-C}_8\text{H}_8\text{-Sc}]_2X$.

As a result, the special Sc-Sc-Sc-Sc bond-chain should also be considered.

$X[\text{Sc-C}_8\text{H}_8\text{-Sc}]X$ complexes are detailed studied by DFT methods, all the optimized structures are local minima. The structural optimization and NBO analysis were carried out using Gaussian 09 program package.¹¹ Bond order values were obtained using Multiwfn program.¹² Table 1 shows the relative energies of singlet and triplet $X[\text{Sc-C}_8\text{H}_8\text{-Sc}]X$ ($X = \text{F, Cl, Br}$). The relative energies of singlet states of $X[\text{Sc-C}_8\text{H}_8\text{-Sc}]X$ are consistently lower compared with their triplet states at different calculated levels. The relative energy of singlet state is 5.9~7.2 kcal/mol lower than triplet state for $X = \text{F}$, 10.0~13.8 kcal/mol lower for $X = \text{Cl}$, and 13.4~14.7 kcal/mol lower for $X = \text{Br}$. Obviously, the singlet states containing Sc-Sc bond are more favourable than the triplet without that. As the calculated results at different levels are generally consistent, only the results obtained at PBEPBE/TZVP level are reported in the following sections.

Table 1 Relative energies (kcal/mol), Sc-Sc distances (Å) and symmetry (tolerance = 0.01) for singlet and triplet states of $X[\text{Sc-C}_8\text{H}_8\text{-Sc}]X$. (*Single-point energies are obtained at PBEPBE/aug-cc-PVTZ//PBEPBE/TZVP level.)

	Calculated level	Relative energies		Sc-Sc distances		Symmetry	
		singlet	triplet	singlet	triplet	singlet	triplet
X=F	PBEPBE/TZVP ¹³	0	7.0	3.262	3.426	D8h	Ci
	CAM-B3LYP/TZVP ¹⁴	0	7.6	3.218	3.414	D8h	Ci
	MPW1PW91/TZVP ¹⁵	0	6.4	3.216	3.464	C2h	C1
	PBEPBE/TZVPP	0	7.2	3.269	3.388	D8h	Ci
	PBEPBE/TZVPD	0	7.2	3.247	3.389	D8h	Ci
	PBEPBE/aug-cc-PVTZ*	0	7.7	3.262	3.426	D8h	Ci
X=Cl	PBEPBE/TZVP	0	13.1	3.186	3.361	D8h	Ci
	CAM-B3LYP/TZVP	0	14.0	3.170	3.341	D8h	Ci
	MPW1PW91/TZVP	0	10.0	3.135	3.581	C2h	C2
	PBEPBE/TZVPP	0	13.8	3.176	3.320	D8h	Ci
	PBEPBE/TZVPD	0	13.6	3.168	3.326	D8h	Ci
	PBEPBE/aug-cc-PVTZ	0	13.8	3.186	3.361	D8h	Ci
X=Br	PBEPBE/TZVP	0	14.2	3.166	3.347	D8h	Ci
	CAM-B3LYP/TZVP	0	15.1	3.150	3.332	D8h	Ci
	MPW1PW91/TZVP	0	14.3	3.118	3.460	C2h	C1
	PBEPBE/TZVPP	0	14.7	3.158	3.307	D8h	Ci
	PBEPBE/TZVPD	0	14.7	3.149	3.312	D8h	Ci
	PBEPBE/aug-cc-PVTZ	0	14.9	3.166	3.347	D8h	Ci

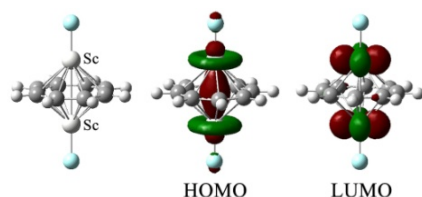


Figure 1 HOMO and LUMO for the singlet $X[\text{Sc-C}_8\text{H}_8\text{-Sc}]X$ ($X = \text{F, Cl, Br}$)

The Sc-Sc distance, the corresponding Mayer bond order and Wiberg bond order of Sc-Sc bond are 3.262 Å, 0.70 and 0.80 for the singlet $\text{F}[\text{Sc-C}_8\text{H}_8\text{-Sc}]\text{F}$; 3.186 Å, 0.71 and 0.81 for the singlet $\text{Cl}[\text{Sc-C}_8\text{H}_8\text{-Sc}]\text{Cl}$, and 3.166 Å, 0.73 and 0.81 for the singlet $\text{Br}[\text{Sc-C}_8\text{H}_8\text{-Sc}]\text{Br}$, respectively. The occupation numbers for the Sc-Sc bonds are 1.847e, 1.847e and 1.846e for $X = \text{F, Cl}$ and Br . According to the bond orders, the Sc-Sc bond in above singlet inverse sandwiches could be classified as single bond. The HOMO and LUMO orbitals of $X[\text{Sc-C}_8\text{H}_8\text{-Sc}]X$ are shown in Figure 1. The HOMO orbital is undoubtedly an σ -bonding molecular orbital with the clear Sc-Sc orbital overlap in the area of the hole of C_8H_8 ligand. The Sc-Sc bonds are mainly composed of d-orbitals (more than 75%) of scandium atoms. The NBO composition for $\sigma_{\text{Sc-Sc}}$ bonds could be described as below:

$$\begin{aligned}\sigma_{\text{Sc-Sc}} &= 0.707(\text{sp}^{0.81}\text{d}^{5.56})\text{Sc} + 0.707(\text{sp}^{0.81}\text{d}^{5.56})\text{Sc} & (X=\text{F}) \\ \sigma_{\text{Sc-Sc}} &= 0.707(\text{sp}^{1.48}\text{d}^{16.16})\text{Sc} + 0.707(\text{sp}^{1.48}\text{d}^{16.16})\text{Sc} & (X=\text{Cl}) \\ \sigma_{\text{Sc-Sc}} &= 0.707(\text{sp}^{1.80}\text{d}^{24.00})\text{Sc} + 0.707(\text{sp}^{1.80}\text{d}^{24.00})\text{Sc} & (X=\text{Br})\end{aligned}$$

Besides, weak Sc-Sc interaction is also found in the triplet $X[\text{Sc-C}_8\text{H}_8\text{-Sc}]X$, the details are provided in Electronic Supplementary Information (ESI).

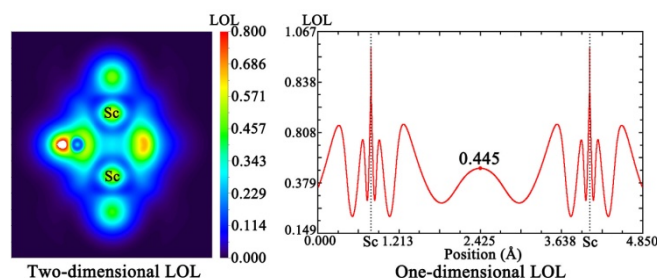


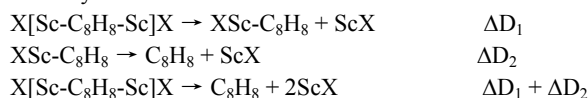
Figure 2 The two-dimensional and one-dimensional LOL plot of the singlet $\text{F}[\text{Sc-C}_8\text{H}_8\text{-Sc}]\text{F}$

The delocalization degree of Sc-Sc bond could be estimated by the Localized Orbital Locator (LOL) value within a range of 0~1.¹⁶ generally high value means the strong localization. Figure 2 describes the two-dimensional and one-dimensional LOL plot of $\text{F}[\text{Sc-C}_8\text{H}_8\text{-Sc}]\text{F}$, the cases of $\text{Cl}[\text{Sc-C}_8\text{H}_8\text{-Sc}]\text{Cl}$ and $\text{Br}[\text{Sc-C}_8\text{H}_8\text{-Sc}]\text{Br}$ are similar. The LOL values in the middle region between two scandium atoms are 0.445 for $X=\text{F}$, 0.488 for $X=\text{Cl}$ and 0.503 for $X=\text{Br}$, respectively. The Sc-Sc bonds could be regarded as delocalized metal-metal bonds. It is noted that from $X=\text{F}$ to $X=\text{Br}$, the singlet-triplet splitting $X[\text{Sc-C}_8\text{H}_8\text{-Sc}]X$ increases gradually from 7.0 kcal/mol to 14.2 kcal/mol, meanwhile, the Sc-Sc distance decreases progressively from 3.262 Å to 3.166 Å. The results indicate the Sc-Sc bond in $\text{Br}[\text{Sc-C}_8\text{H}_8\text{-Sc}]\text{Br}$ would be more favourable than those in $\text{F}[\text{Sc-C}_8\text{H}_8\text{-Sc}]\text{F}$ and $\text{Cl}[\text{Sc-C}_8\text{H}_8\text{-Sc}]\text{Cl}$. The HOMO-

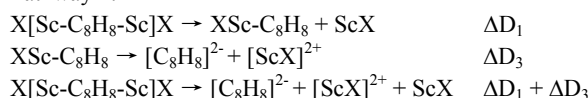
LUMO gaps for $X = \text{F, Cl}$ and Br of $X[\text{Sc-C}_8\text{H}_8\text{-Sc}]X$ are 0.79, 1.08 and 1.13 eV, respectively. These values give a rough estimate that the molecules might be electro-conductive.¹⁷

The stability of Sc-Sc bond in singlet $X[\text{Sc-C}_8\text{H}_8\text{-Sc}]X$ ($X = \text{F, Cl, Br}$) against the dissociation is considered as well. The dissociation reactions of $X[\text{Sc-C}_8\text{H}_8\text{-Sc}]X$ with respect to produce neutral C_8H_8 and ScX with $\text{Sc}(\text{I})$ (Pathway 1) or charged $[\text{C}_8\text{H}_8]^{2-}$ anion, $[\text{ScX}]^{2+}$ with $\text{Sc}(\text{III})$ and ScX (Pathway 2), are represented as below:

Pathway 1:



Pathway 2:



The dissociation energies of singlet $X[\text{Sc-C}_8\text{H}_8\text{-Sc}]X$ ($X = \text{F, Cl, Br}$) are shown in Table 2. Both the two pathways are endothermic. Pathway 1 needs lower dissociation energies compared with Pathway 2: for the first step, $X[\text{Sc-C}_8\text{H}_8\text{-Sc}]X$ dissociates into $X\text{Sc-C}_8\text{H}_8$ and ScX (ScX is open-shell singlet), for the second step, $X\text{Sc-C}_8\text{H}_8$ dissociates into C_8H_8 and ScX . The first dissociation energy ΔD_1 and the total dissociation energy $\Delta D_1 + \Delta D_2$ for $\text{F}[\text{Sc-C}_8\text{H}_8\text{-Sc}]\text{F}$, $\text{Cl}[\text{Sc-C}_8\text{H}_8\text{-Sc}]\text{Cl}$, and $\text{Br}[\text{Sc-C}_8\text{H}_8\text{-Sc}]\text{Br}$ are 30.3 and 157.1, 51.0 and 184.3, and 48.9 and 177.5 kcal/mol, respectively. Therefore, these inverse sandwiches with particular metal-metal bonds could be stable against the dissociation process, especially for $X = \text{Cl}$ and Br .

Table 2 The dissociation energies (kcal/mol) of singlet $X[\text{Sc-C}_8\text{H}_8\text{-Sc}]X$ ($X = \text{F, Cl, Br}$) at PBEPBE/TZVP level with BSSE or ZPE (zero-point energy) corrections, and at CAM-B3LYP/TZVP level

	ΔD_1	ΔD_2	ΔD_3	$\Delta D_1 + \Delta D_2$	$\Delta D_1 + \Delta D_3$
PBEPBE/TZVP					
$\text{F}[\text{Sc-C}_8\text{H}_8\text{-Sc}]\text{F}$	30.3	126.8	673.1	157.1	703.4
$\text{Cl}[\text{Sc-C}_8\text{H}_8\text{-Sc}]\text{Cl}$	51.0	133.3	659.0	184.3	710.0
$\text{Br}[\text{Sc-C}_8\text{H}_8\text{-Sc}]\text{Br}$	48.9	128.6	648.8	177.5	697.7
with BSSE corrections					
$\text{F}[\text{Sc-C}_8\text{H}_8\text{-Sc}]\text{F}$	27.6	117.3	668.1	144.9	695.7
$\text{Cl}[\text{Sc-C}_8\text{H}_8\text{-Sc}]\text{Cl}$	48.3	132.7	652.8	181.0	701.1
$\text{Br}[\text{Sc-C}_8\text{H}_8\text{-Sc}]\text{Br}$	46.5	126.5	643.2	173.0	689.7
with ZPE corrections					
$\text{F}[\text{Sc-C}_8\text{H}_8\text{-Sc}]\text{F}$	30.9	124.1	665.2	155.0	696.1
$\text{Cl}[\text{Sc-C}_8\text{H}_8\text{-Sc}]\text{Cl}$	50.8	130.7	651.1	181.5	701.9
$\text{Br}[\text{Sc-C}_8\text{H}_8\text{-Sc}]\text{Br}$	48.7	126.1	641.0	174.8	689.7
CAM-B3LYP/TZVP					
$\text{F}[\text{Sc-C}_8\text{H}_8\text{-Sc}]\text{F}$	13.3	113.2	675.3	126.5	688.6
$\text{Cl}[\text{Sc-C}_8\text{H}_8\text{-Sc}]\text{Cl}$	33.4	118.2	665.2	151.6	698.6
$\text{Br}[\text{Sc-C}_8\text{H}_8\text{-Sc}]\text{Br}$	36.4	118.5	656.8	154.9	693.2

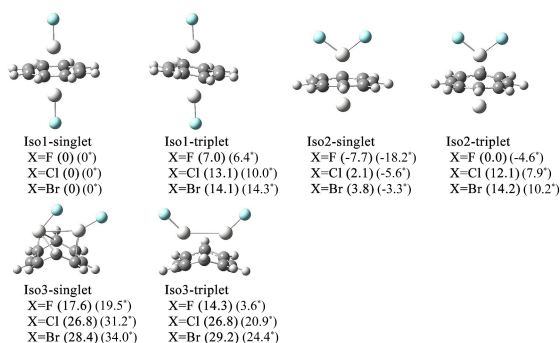


Figure 3 Structures and relative energies of the isomers for $\text{Sc}_2\text{C}_8\text{H}_8\text{X}_2$ at PBEPBE/TZVP level and CAM-B3LYP/TZVP level (with * symbol)

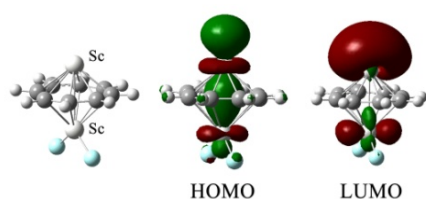


Figure 4 HOMO and LUMO for the singlet $\text{Sc-C}_8\text{H}_8\text{-ScX}_2$ ($\text{X} = \text{F}, \text{Cl}, \text{Br}$)

Figure 3 describes the relative energies and structures for $\text{Sc}_2\text{C}_8\text{H}_8\text{X}_2$ ($\text{X} = \text{F}, \text{Cl}, \text{Br}$) isomers. At PBEPBE/TZVP level, the Iso2-singlet is the lowest in energy for $\text{Sc}_2\text{C}_8\text{H}_8\text{F}_2$, while the Iso1-singlet isomers of $\text{Sc}_2\text{C}_8\text{H}_8\text{Cl}_2$ and $\text{Sc}_2\text{C}_8\text{H}_8\text{Br}_2$ are ground states. At CAM-B3LYP/TZVP level, although the Iso2-singlet isomers are the lowest in energy, very small energy differences are between Iso1-singlet and Iso2-singlet isomers for $\text{Sc}_2\text{C}_8\text{H}_8\text{Cl}_2$ and $\text{Sc}_2\text{C}_8\text{H}_8\text{Br}_2$. Thus, both of the Iso1-singlet and Iso2-singlet isomers have the possibility to exist. The HOMO and LUMO orbitals for the Iso2-singlet isomers of $\text{Sc}_2\text{C}_8\text{H}_8\text{X}_2$ ($\text{X} = \text{F}, \text{Cl}, \text{Br}$), which could be termed as another inverse sandwich $[\text{Sc-C}_8\text{H}_8\text{-Sc}]_2\text{X}_2$, are shown in Figure 4. An apparent σ -bonding with Sc-Sc orbital overlap is found in the area of the hole of C_8H_8 ligand. The Sc-Sc distance, the corresponding Mayer bond order and Wiberg bond order of Sc-Sc bond in Iso2-singlet isomers at PBEPBE/TZVP level are 3.275 Å, 0.56 and 0.58 for $\text{X}=\text{F}$; 3.216 Å, 0.68 and 0.68 for $\text{X}=\text{Cl}$, and 3.203 Å, 0.70 and 0.70 for $\text{X}=\text{Br}$, respectively. The results indicate that the low-energy isomers, no matter in the form of $\text{X}[\text{Sc-C}_8\text{H}_8\text{-Sc}]_2\text{X}$ or $[\text{Sc-C}_8\text{H}_8\text{-Sc}]_2\text{X}_2$, all possess the inverse sandwich structures with Sc-Sc bond through the C_8H_8 ligand.

Table 3. Relative energies (kcal/mol) and Sc-Sc distances (Å) for singlet and triplet states of $\text{X}[\text{Sc-C}_8\text{H}_8\text{-Sc}]_2\text{X}$ ($\text{X} = \text{F}, \text{Cl}, \text{Br}$) at PBEPBE/TZVP level

	Sc1-Sc2	Sc3-Sc4	Sc2-Sc3	Relative energies
X = F, singlet	3.225	3.225	3.294	0
X = F, triplet	3.309	3.309	2.985	7.2
X = Cl, singlet	3.192	3.192	3.327	0
X = Cl, triplet	3.281	3.281	3.020	9.1
X = Br, singlet	3.185	3.185	3.326	0
X = Br, triplet	3.275	3.275	3.023	9.5

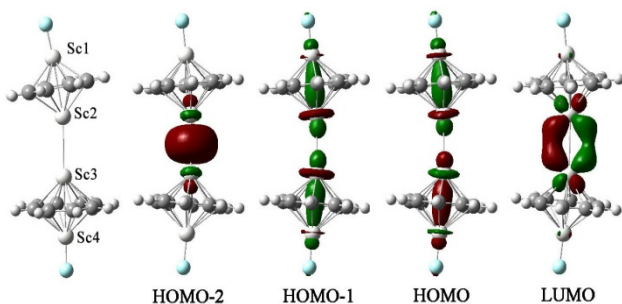


Figure 5 HOMO and LUMO for the singlet $\text{X}[\text{Sc-C}_8\text{H}_8\text{-Sc}]_2\text{X}$ ($\text{X} = \text{F}, \text{Cl}, \text{Br}$)

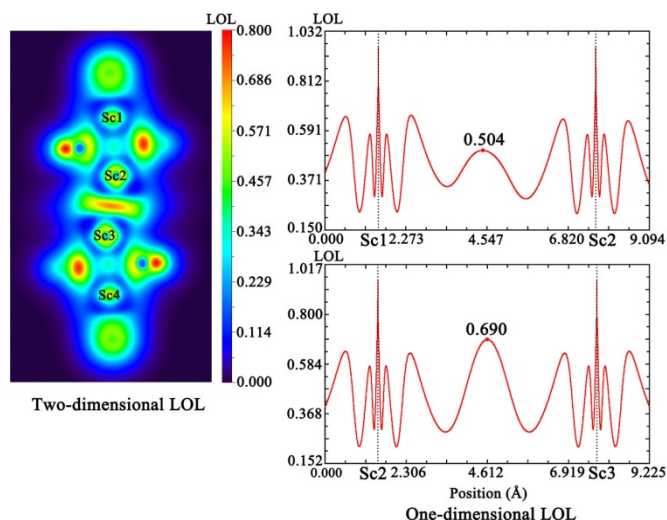


Figure 6. The two-dimensional and one-dimensional LOL plot of the singlet $\text{F}[\text{Sc-C}_8\text{H}_8\text{-Sc}]_2\text{F}$

To further understand the Sc-Sc bond in more complicated coordination complexes, $\text{X}[\text{Sc-C}_8\text{H}_8\text{-Sc}]_2\text{X}$ ($\text{X} = \text{F}, \text{Cl}, \text{Br}$) with two $[\text{Sc-C}_8\text{H}_8\text{-Sc}]$ units are calculated. Table 3 lists the relative energies and Sc-Sc distances. The singlet states are more stable in energy than the triplet states. Figure 5 shows the HOMO and LUMO orbitals for singlet $\text{X}[\text{Sc-C}_8\text{H}_8\text{-Sc}]_2\text{X}$, where Sc1-Sc2 and Sc3-Sc4 represent the Sc-Sc bonds passing through C_8H_8 ligand, Sc2-Sc3 represents the direct Sc-Sc bonds between two $[\text{Sc-C}_8\text{H}_8\text{-Sc}]$ units. Molecular orbitals indicate Sc1-Sc2, Sc3-Sc4 and Sc2-Sc3 are all σ -bonding with Sc-Sc orbital overlap. By means of Mayer bond order and Wiberg bond order, these Sc-Sc bonds could also be classified as single bonds. The Sc1-Sc2 (Sc3-Sc4) bond is mainly composed of d-orbitals of scandium atoms, while the Sc2-Sc3 is primarily composed of s-orbitals. The NBO composition for $\sigma_{\text{Sc-Sc}}$ bonds could be described as follows:

$$\begin{aligned}
 \sigma_{\text{Sc1-Sc2}} &= 0.678(\text{sp}^{1.17}\text{d}^{8.28})_{\text{Sc1}} + 0.735(\text{sp}^{1.29}\text{d}^{34.33})_{\text{Sc2}} & (\text{X}=\text{F}) \\
 \sigma_{\text{Sc2-Sc3}} &= 0.707(\text{sp}^{0.27}\text{d}^{0.11})_{\text{Sc2}} + 0.707(\text{sp}^{0.27}\text{d}^{0.11})_{\text{Sc3}} & (\text{X}=\text{F}) \\
 \sigma_{\text{Sc1-Sc2}} &= 0.714(\text{sp}^{1.57}\text{d}^{20.23})_{\text{Sc1}} + 0.700(\text{sp}^{1.79}\text{d}^{35.66})_{\text{Sc2}} & (\text{X}=\text{Cl}) \\
 \sigma_{\text{Sc2-Sc3}} &= 0.707(\text{sp}^{0.30}\text{d}^{0.11})_{\text{Sc2}} + 0.707(\text{sp}^{0.30}\text{d}^{0.11})_{\text{Sc3}} & (\text{X}=\text{Cl}) \\
 \sigma_{\text{Sc1-Sc2}} &= 0.720(\text{sp}^{1.99}\text{d}^{28.25})_{\text{Sc1}} + 0.694(\text{sp}^{1.74}\text{d}^{38.27})_{\text{Sc2}} & (\text{X}=\text{Br}) \\
 \sigma_{\text{Sc2-Sc3}} &= 0.707(\text{sp}^{0.30}\text{d}^{0.11})_{\text{Sc2}} + 0.707(\text{sp}^{0.30}\text{d}^{0.11})_{\text{Sc3}} & (\text{X}=\text{Br})
 \end{aligned}$$

The distances of Sc1-Sc2 and Sc3-Sc4 for singlet $\text{X}[\text{Sc-C}_8\text{H}_8\text{-Sc}]_2\text{X}$ ($\text{X} = \text{F}, \text{Cl}, \text{Br}$) are all shorter than the distances of Sc2-Sc3, in other words, the Sc-Sc bonds passing through C_8H_8 ligand are stronger than the direct Sc-Sc bonds between two $[\text{Sc-C}_8\text{H}_8\text{-Sc}]$ units. Figure 6 describes LOL plot of $\text{F}[\text{Sc-C}_8\text{H}_8\text{-Sc}]_2\text{F}$, the cases of $\text{Cl}[\text{Sc-C}_8\text{H}_8\text{-Sc}]_2\text{Cl}$ and $\text{Br}[\text{Sc-C}_8\text{H}_8\text{-Sc}]_2\text{Br}$ are similar. The LOL values in the middle region of the Sc1-Sc2 and Sc2-Sc3 bonds are 0.504 and 0.690 for $\text{X}=\text{F}$, 0.514 and 0.709 for $\text{X}=\text{Cl}$, and 0.519 and 0.710 for $\text{X}=\text{Br}$, respectively. Compared with the delocalized Sc1-Sc2 (Sc3-Sc4) bond, the Sc2-Sc3 bond is more localized. The HOMO-LUMO gaps for $\text{X} = \text{F}, \text{Cl}$ and Br of $\text{X}[\text{Sc-C}_8\text{H}_8\text{-Sc}]_2\text{X}$ are 0.65, 0.74 and 0.75 eV, which are much smaller than the 0.79, 1.08 and 1.13 eV for $\text{X}[\text{Sc-C}_8\text{H}_8\text{-Sc}]_2\text{X}$. Therefore, better conductivity would be for the former than the latter.

The uninterrupted Sc1-Sc2-Sc3-Sc4 bond-chain in $X[\text{Sc-C}_8\text{H}_8\text{-Sc}]_n\text{X}$ ($X = \text{F, Cl, Br}$) might be particularly interesting for the field of materials chemistry. Suppose some more complicated complex $X[\text{Sc-C}_8\text{H}_8\text{-Sc}]_n\text{X}$ containing similar constant -Sc-Sc- metallic bond-chain with small HOMO-LUMO gap, it is of great interest whether the constant linear metal-metal bonds make it a potential functional material.

In summary, Sc-Sc bond passing through the ligand is predicted to be favourable in $X[\text{Sc-C}_8\text{H}_8\text{-Sc}]\text{X}$ ($X = \text{F, Cl, Br}$). The unique Sc-Sc bond is formed an σ -bonding with the clear Sc-Sc orbital overlap in the area of the hole of C_8H_8 ligand. The Sc-Sc bond strengthens followed by the increase of the atomic number of halogen element from F to Br. The complex $X[\text{Sc-C}_8\text{H}_8\text{-Sc}]_2\text{X}$ ($X = \text{F, Cl, Br}$) includes both the Sc-Sc bond passing through C_8H_8 ligand, and the direct Sc-Sc bond between two $[\text{Sc-C}_8\text{H}_8\text{-Sc}]$ units. The main reason of Sc-Sc bond passing through the ligand in $X[\text{Sc-C}_8\text{H}_8\text{-Sc}]\text{X}$ or $[\text{Sc-C}_8\text{H}_8\text{-Sc}]$ unit might be attributed to two fields. On the one hand, the Sc-Sc distance could be shortened a certain range for bonding because of the electrostatic attraction and coordination between scandium atoms with arene ligand. On the other hand, the electronic repulsion between two scandium atoms could be greatly reduced due to the scandium atoms on opposite sides of the arene ligand. Besides, the particular shape of d_{z^2} orbital of transition metal might be very comfortable to stick into the hole of arene and form the metal-metal bond passing through the ligand.

Methodology

The structural optimization and NBO analysis were carried out using Gaussian 09 program package. Harmonic vibrational frequencies are calculated to insure the correct local minima. As the calculated results of singlet and triplet states of $X[\text{Sc-C}_8\text{H}_8\text{-Sc}]\text{X}$ are calculated at MPW1PW91/TZVP, CAM-B3LYP/TZVP, PBEPBE/TZVP, PBEPBE/TZVPP, PBEPBE/TZVPD and PBEPBE/aug-cc-PVTZ//PBEPBE/TZVP levels are consistent, only the results obtained at PBEPBE/TZVP level are reported in the other sections. The dissociation energies are calculated at PBEPBE/TZVP and CAM-B3LYP/TZVP levels, the BSSE and ZPE (zero-point energy) corrections are also considered at PBEPBE/TZVP level. Bond order values and Localized Orbital Locator plot were obtained using Multiwfn program at PBEPBE/TZVP level. Further structural details are presented in Supporting Information.

Acknowledgements

This work is supported by the National Natural Science Foundation of China (No. 21273093, 21301041, 51476049), and the Natural Science Foundation of Heilongjiang Province of China (No. B201409).

Notes and references

^a Chemistry Center, College of Food Engineering, Harbin University of Commerce, Harbin 150076, People's Republic of China. Fax: 86-451-84844281; Tel: 86-451-84844281; E-mail: liunann.yl@gmail.com

^b State Key Laboratory of Theoretical and Computational Chemistry, Institute of Theoretical Chemistry, Jilin University, Changchun 130023, People's Republic of China. Fax: 86-431-88498026; Tel: 86-431-88498023; E-mail: yhdd@jlu.edu.cn

- B. Buchin, C. Gemel, T. Cadenbach, R. Schmid, R. A. Fischer, *Angew. Chem. Int. Ed.* 2006, **45**, 1074-1076.
- S. Kriek, H. Goerls, L. Yu, Ma. Reiher, M. Westerhausen, *J. Am. Chem. Soc.* 2009, **131**, 2977-2985.
- D. Patel, F. Moro, J. McMaster, W. Lewis, A. J. Blake, S. T. Liddle, *Angew. Chem. Int. Ed.* 2011, **50**, 10388-10392.
- W. H. Monillas, G. P. A. Yap, L. A. MacAdams, K. H. Theopold, *J. Am. Chem. Soc.* 2007, **129**, 8090-8091
- G. B. Nikiforov, P. Crewdson, S. Gambarotta, I. Korobkov, P. H. M. Budzelaar, *Organometallics*. 2007, **26**, 48-55.
- A. P. Sergeeva, A. I. Boldyrev, *Organometallics*. 2010, **29**, 3951-3954.
- K. Hatua, P. K. Nandi, *J Mol Model*. 2014, doi: 10.1007/s00894-014-2440-0
- N. N. Liu, S. M. Gao, Y. H. Ding, *Dalton Trans.* 2014, DOI: 10.1039/C4DT02282C
- I. Fernández, E. Cerpa, G. Merino, G. Frenking, *Organometallics*. 2008, **27**, 1106-1111.
- N. N. Liu, J. Xu, Y. H. Ding, *Int. J. Quantum. Chem.* 2013, **113**, 1018-1025.
- Gaussian 09, Revision A.1, M. J. Frisch, G. W. Trucks, H. B. Schlegel, G. E. Scuseria, M. A. Robb, J. R. Cheeseman, G. Scalmani, V. Barone, B. Mennucci, G. A. Petersson, H. Nakatsuji, M. Caricato, X. Li, H. P. Hratchian, A. F. Izmaylov, J. Bloino, G. Zheng, J. L. Sonnenberg, M. Hada, M. Ehara, K. Toyota, R. Fukuda, J. Hasegawa, M. Ishida, T. Nakajima, Y. Honda, O. Kitao, H. Nakai, T. Vreven, J. A. Montgomery, Jr., J. E. Peralta, F. Ogliaro, M. Bearpark, J. J. Heyd, E. Brothers, K. N. Kudin, V. N. Staroverov, R. Kobayashi, J. Normand, K. Raghavachari, A. Rendell, J. C. Burant, S. S. Iyengar, J. Tomasi, M. Cossi, N. Rega, J. M. Millam, M. Klene, J. E. Knox, J. B. Cross, V. Bakken, C. Adamo, J. Jaramillo, R. Gomperts, R. E. Stratmann, O. Yazyev, A. J. Austin, R. Cammi, C. Pomelli, J. W. Ochterski, R. L. Martin, K. Morokuma, V. G. Zakrzewski, G. A. Voth, P. Salvador, J. J. Dannenberg, S. Dapprich, A. D. Daniels, O. Farkas, J. B. Foresman, J. V. Ortiz, J. Cioslowski, and D. J. Fox, Gaussian, Inc., Wallingford CT, 2009.
- T. Lu, F. Chen, *J. Comp. Chem.* 2012, **33**, 580-592.
- a) J. P. Perdew, K. Burke, and M. Ernzerhof, *Phys. Rev. Lett.* 1996, **77**, 3865-3868; b) J. P. Perdew, K. Burke, and M. Ernzerhof, *Phys. Rev. Lett.* 1997, **78**, 1396.
- T. Yanai, D. P. Tew, N. C. Handy, *Chem. Phys. Lett.* 2004, **393**, 51-57.
- a) C. Adamo, V. Barone, *J. Chem. Phys.* 1998, **108**, 664-675; b) J. P. Perdew, J. A. Chevary, S. H. Vosko, K. A. Jackson, M. R. Pederson, D. J. Singh, C. Fiolhais, *Phys. Rev. B*. 1992, **46**, 6671-6687.
- (a) H. L. Schmider, A. D. Becke, *J. Mol. Struct. (THEO)*. 2000, **527**, 51-61. (b) C. Gatti, *Z. Kristallogr.* 2005, **220**, 399-457.
- (a) D. K. Seo, R. Hoffmann, *Theor. Chem. Acc.* 1999, **102**, 23-32; (b) P. Batail, *Chem. Rev.* 2004, **104**, 4887-4890.